Journal of Marine Science and Technology, Vol. 25, No. 3, pp. 259-267 (2017)
DOI: 10.6119/JMST-016-1214-1

ZINC-RICH LITHIUM SILICATE COATINGS FOR CORROSION PREVENTION IN STEELS

Jiang-Jhy Chang[1], Wei-Chung Yeih[1], Kuo-Lien Chen[1], and Maochieh Chi[2]

Key words: zinc, lithium silicate, coating, corrosion prevention.

ABSTRACT

In this study, we investigated the properties of zinc-rich lithium silicate coatings using various moduli of lithium silicate and zinc powder ratios, which are defined as the mass ratios of zinc powder over lithium silicate. Coating properties examined included film-forming ability, workability, mechanical behavior, resistance to highly alkali or acid solutions, and weather resistance (ultraviolet exposure test). The results showed that the zinc powder ratio significantly influenced workability and film-forming ability. When the zinc powder ratio of the coating was low, the coating delaminated and cracked. When the zinc powder ratio was high, the workability of the coating was found to be poor; the coating was observed to be sticky and hard to mix; thus, applying a uniform layer of coating on the steel substrate was difficult. Additionally, the modulus of lithium silicate affected the mechanical performance of the coating as well as cathodic protection capability. A coating using a lower modulus yielded a coating of more desirable thickness, hardness, viscosity, and adhesive property. In addition, the cathodic protection lasted longer.

I. INTRODUCTION

Steels possess excellent mechanical properties and are often used in construction engineering. However, steels corrode naturally according to thermodynamics; thus, preventing such corrosion is a crucial task for engineers. Many techniques have been developed to prevent steel corrosion, including coating or painting. Coating creates a physical barrier preventing hazardous species from coming into contact with the steel. Coatings are of two types: organic and inorganic. Although organic coatings have been used for a long time, they have several drawbacks. One is that volatile organic compounds in organic coatings are harmful to humans and, because they generate global-warming gases, to the environment as well (Marchebois et al., 2002). Another is the aging of organic coatings exposed to ultraviolet radiation from the sun, necessitating special techniques to enhance their ultraviolet resistance (e.g., Chen et al., 2006).

Unlike organic coatings, inorganic coatings are environmentally friendly and possess ultraviolet resistance. The properties of these inorganic coatings have been reviewed (Sidkey and Hocking, 1999). Among the various inorganic coatings, lithium silicate coatings, particularly zinc-rich lithium silicate coatings, were the focus of this study. The reasons for selecting zinc-rich lithium silicate coatings are as follows:

(1) Zinc-silicate-zinc and zinc-silicate-iron compounds are solid structures that yield strong mechanical behaviors between coating and metal;
(2) Zinc may play the role of a sacrificial anode, thereby inhibiting corrosion.

Several related articles about this type of coating are summarized as follows.

Silicates have been used in coatings because of their excellent performance. Weldes and Lange (1969) reviewed the properties of soluble silicates. Parashar et al. (2001) found that ethyl silicate binders to yield high-performance coatings. Parashar et al. (2003) observed that the performances of water-borne nontoxic inorganic silicate coatings depended on the ratio of silica to alkali metal oxide. They revealed that the drying rate and chemical resistance of the film increased with the ratio of silica to alkali metal oxide, but the water miscibility of the system decreased. Parashar et al. (2001, 2003) reported the film-forming process in zinc-rich lithium silicates. First, the carbon dioxide dissolves in water and yields carbonic acid, which participates in the following reaction:

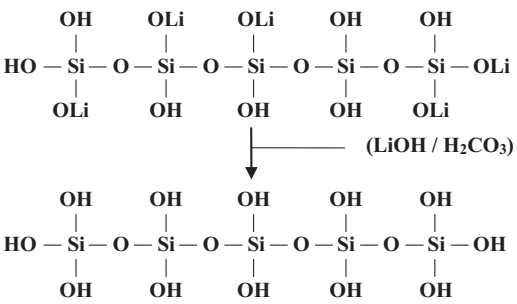

(1)

Paper submitted 05/11/15; revised 11/02/15; accepted 12/14/16. Author for correspondence: Wei-Chung Yeih (e-mail: wcyeih@ntou.edu.tw).
[1] Department of Harbor and River Engineering, National Taiwan Ocean University, Keelung, Taiwan, R.O.C.
[2] Department of Fire Science, WuFeng University, Chiayi, Taiwan, R.O.C.

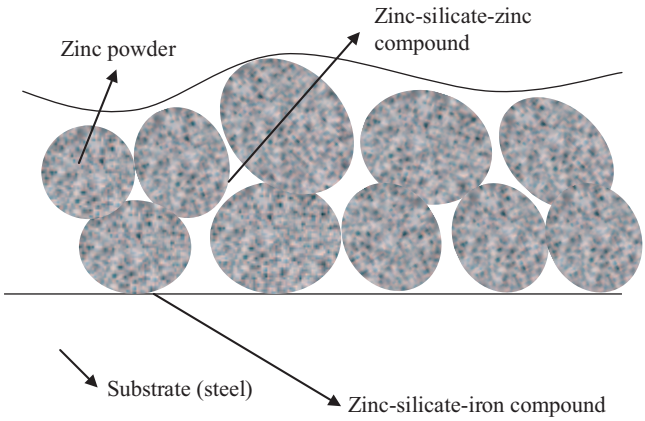

Fig. 1. Crosslinking effects generated zinc-silicate-zinc compounds and zinc-silicate-iron compounds.

The cross-linking reaction occurs

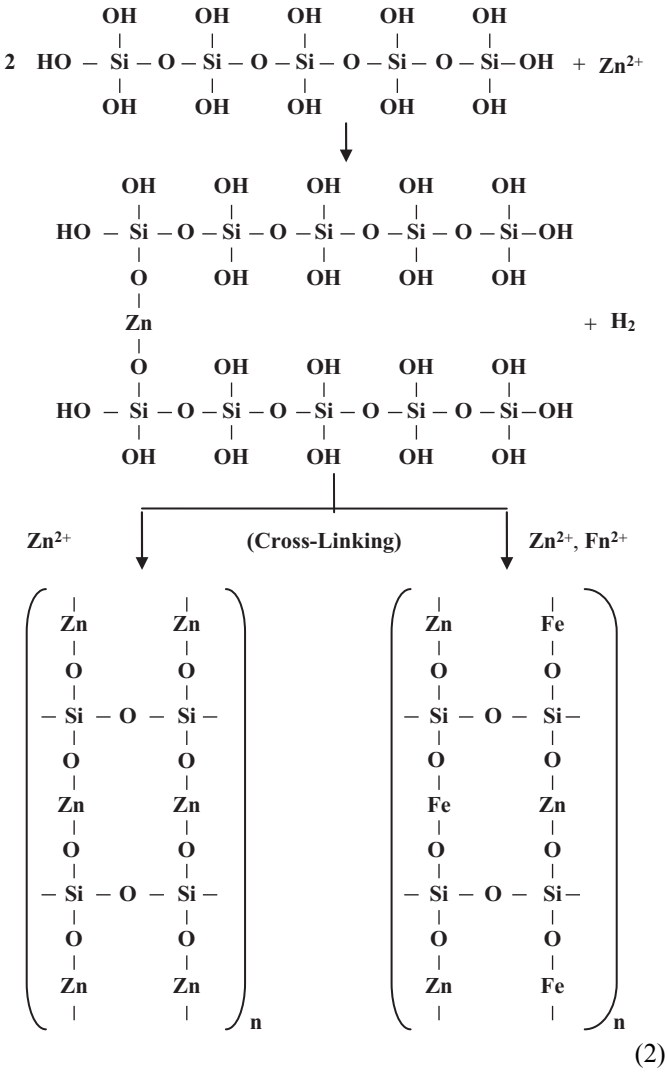

(2)

Consequently, a solid film with zinc-silicate-zinc and zinc-silicate-iron compounds is generated (Fig. 1).

Oostendorp et al. (1992) reported that the hydrolysis and alcoholysis of alkoxysilanes are of interest regarding the use of silane-coupling agents as adhesion promoters, the preparation of zinc-rich silicate coatings, the sol-gel process, and the preparation of silicones in general. Canosa et al. (2012) developed environmentally friendly, nanostructured inorganic coatings suitable for the protection of metal substrates. Cruz et al. (2006) reported that lithium silicate has excellent thermal stability. Pfeiffer et al. (1998) reported that lithium silicates could be synthesized using three techniques: solid state reaction, the precipitation method, and the sol-gel method. Kumar et al. (2009) studied the effect of NiO on phase formation and concluded that the addition of NiO favored the interdiffusion of species at the interface, leading to superior sealing.

Current anticorrosive-coating technology aims to make products that control the development of electrode reactions and that isolate the metal surface by the application of films with low permeability and high adhesion (Sorensen et al., 2011). Zinc-rich coatings and those modified with extenders and/or metal corrosion inhibitors display higher efficiency compared with coatings rich in other metals. However, because metallic zinc is extremely reactive, manufacturers generally formulate zinc coatings in two packages, which implies that zinc must first be incorporated into the vehicle before being used as a coating application (Giudice, 2012).

Coatings consisting of high-purity zinc dust dispersed in organic and inorganic vehicles have been designed in view of the use of zinc as a sacrificial anode (cathodic protection) (Veritas, 2010). The anodic reaction corresponds to the oxidation of zinc particles (loss of electrons), whereas the cathodic reaction generally involves oxygen reduction (gain of electrons) on the surface of iron or steel. The electrons released by zinc prevent or control the oxidation of the metal substrate. Theoretically, the role of the protective mechanism is similar to that of a continuous layer of zinc applied by galvanizing, though differences exist, such as the initial porosity of the coating film (Jegannathan et al., 2006).

In immersion conditions, the time of protection depends on the zinc content in the film and on its dissolution rate. The mechanism differs for films exposed to the atmosphere, because after cathodic protection in the first stage, the action is restricted substantially to a barrier effect (inhibition resistance) generated by the soluble zinc salts from corrosion, which seals the pores and thereby controls access to water, water vapor, and various pollutants (Hammouda et al., 2011).

The durability and protective ability of a coating depends on, in addition to environmental factors, the relationship between the permeability of the film during the first stage of exposure and the cathodic protection that occurs (Giudice, 2012). In outdoor exposure, the time required for satisfactory inhibitory action may be higher because of the polarizing effect of the corrosion products of zinc (Pedersen et al., 2009).

The main goal of this study was to investigate the moduli of lithium silicate (m) and zinc powder ratio on the performance of zinc-rich lithium silicate coatings. Lithium silicate contains

LiOH solution and silicate sol, expressed as Li_2O *m* SiO_2, where *m* is the moduli of lithium silicate. Hare (1998) reported *m* to be in the range of 2.1-8.5. We performed immersion tests, open circuit potential tests, scanning electron microscopy, energy dispersion spectrum tests, and X-ray diffraction to evaluate the performance of the zinc-rich lithium silicate coatings on the basis of the following parameters: drying time, coating thickness, coating appearance, hardness, adhesion, and weather resistance upon exposure to ultraviolet light.

The remainder of this paper is organized as follows. The materials used and experiments conducted in this study are discussed in Section 2. The results and discussion are presented in Section 3. Conclusions are presented in Section 4.

II. MATERIALS AND EXPERIMENTS

1. Two-Stage Study

This study comprised two stages. In the first stage, we fabricated coatings with the following mixing variables: (i) *m* values of 4, 5, 6, 7, 10, 15, and 30 and (ii) zinc powder ratios of 2, 3.5, 5, and 6.5. The appropriate range of moduli of lithium silicate has been proposed previously; in this study, we selected four moduli within this region (4, 5, 6, and 7) and four moduli exceeding this region (10, 15 and 30) to examine their performance and thereby verify the region suggested in the literature. The zinc powder ratios were selected according to primary trials and comprised one optimal ratio (5), two low ratios (2 and 3.5), and one high ratio (6.5).

The zinc powder we used had a specific weight of 7.14, a particle size of 7-9 μm, and a purity of 99%. The steel plate we used was of SS400 structural steel with a yield strength of > 245 MPa and a tensile strength of 500 MPa.

These coatings were evaluated on the basis of their workability, film-forming ability, mechanical properties, and corrosion prevention ability. After the first stage, several zinc-rich lithium silicate coatings with superior performance were selected for the subsequent experiments.

In the second stage of the study, the variable for the zinc-rich lithium silicate coatings was the number of painted layers. Steel plates were coated with different layers of these selected zinc-rich lithium silicate coatings and compared with a control specimen (a steel plate without any coating) and an epoxy-coated steel plate. In addition, the performance of coatings while the scratch exits was studied by making an X-shaped scratch on the coating. Weather resistance (ultraviolet exposure) and corrosion tests were conducted to evaluate the performance of these coatings.

We labeled the experimental specimens by using three codes. The code began with 4, 5, 6, 7, 10, 15, or 30, which represented *m*, with E for the epoxy coating and O for the control specimen (without coating). The following character in the code was a, b, or c, which represented the number of layers of the zinc-rich lithium silicate coating of 1, 2, and 3; or X for X-shaped scratch on coating. Next in the code was 2, 3.5, 5, or 6.5, which indicated the zinc powder ratio. For example, "4a5" would represent a zinc-rich lithium silicate coating with a modulus of four, one coating layer, and a zinc powder ratio of 5.

2. Experiments

Steel plates of 15 × 10 × 0.1 cm were polished and used as the substrate to be protected. Before the coating process, rust on the surface of the steel plates was removed using a grinder until the metallic luster was observed; grease on the surface was removed using acetone. The surface preparing process was completed by washing the plates with water and drying in an oven. Subsequent subsections discuss the tests performed on the coated specimens.

1) Mixing Capability

The mixing capability of the zinc-rich lithium silicate was evaluated using Chinese National Standard (CNS) 14132. The designated quantity of zinc powder was mixed with lithium silicate by using a glass stirrer; the mixture was evaluated as "easy to mix" if no agglomeration or segregation was observed according to CNS 14132.

2) Flowability Test

A flowability test was conducted to evaluate the workability of the coating materials: The flowability of a coating was considered inversely proportional to the difficulty of the coating process. A 2-mL dosage of the coating material was poured on an acrylic wedge inclined at an angle of 30°; the time the coating material took to travel 20 cm was recorded. A shorter travel time indicated higher flowability.

3) Painting Workability

The painting method mentioned in CNS 9007 was adopted. The polished steel plate was placed flat on a level surface. The plate was painted first along its length, second along its breadth, and finally along its length again. The overlapping distance between two adjacent brush strokes was approximately 10 mm. If no difficulty was encountered during the painting process, the coating material was considered "not obstructive to the painting processes," according to CNS 14132.

4) Coating Thickness

The coating thickness was measured using an electromagnetic thickness meter with (i) an accuracy of ± 1 μm for thicknesses of < 50 μm and ± 2 μm for thicknesses of > 50 μm and (ii) a resolution of 0.1 μm for thicknesses of < 100 μm and 1 μm for thicknesses of > 100 μm. Coating thickness was calculated using the mean of five successive measurements on the plate. The distance between the measuring spot and any edge was at least 10 mm.

5) Drying Time

Drying time was evaluated using CNS 10756. The drying time of the *half stiff and dry state* was considered achieved when no scratch mark could be found by scratching the middle point of the coating with a fingernail.

6) Adhesive Capability Test

The adhesive capability between the coating and the steel substrate was evaluated using the adhesive strength test and X-cutting adhesive tape method. The adhesive strength test was performed using the following steps:

1. A steel head was attached to the steel plate by using an adhesive agent.
2. The plate was placed at room temperature for 24 h.
3. The coating on the plate was cut along the head edge to ensure that the area of applied force was fixed.
4. A pull-off test was performed and the maximum loading was recorded.
5. Dividing the maximum loading by the area, we calculated the adhesive strength.

The X-cutting adhesive tape method was performed using the following steps:

1. Two straight line cuttings were made through the coating in the middle of the plate. The intersection angle between the two cutting lines was 30° and the length of the cutting line was 40 mm.
2. Two adhesive 50-mm-long strips of tape were used to cover the cutting lines. Pressure was exerted to ensure adhesion of the tape to the coating.
3. After 2-3 min, the two strips were removed simultaneously from the surface quickly.
4. After removing the tape, a visual inspection of the coating around the X-shaped cutting lines was made.
5. The evaluation points were made according to CNS 10757.

7) Appearance Evaluation

After coating, the plate was placed at room temperature for 48 h. The appearance of the coating was evaluated through visual inspection according to CNS 10756-1. The following defects of appearance were recorded: nonuniform and nonsmooth appearance, chaps, bursts, blisters, rill marks, and uneven heights.

8) Hardness Determined Using the Vickers Hardness Test

The hardness of the coating was evaluated using the Vickers hardness test. The Vickers pyramid number (HV), also called the diamond pyramid hardness, was calculated as follows:

$$HV = 2\,P\sin(\theta/2)/d^2 = 1.8544\,P/d^2 \qquad (3)$$

where P is the force applied to the diamond in kilograms-force, θ is the angle of the intersection (136°) between two tangents to the circle at the ends of a chord $3d/8$ long, and d is the average length of the diagonal left by the indenter in millimeters. Therefore, HV in Eq. (3) takes the unit kilograms-force/mm^2.

9) Hardness Evaluation by Use of Pencils

The hardness of the coating was also evaluated using pencils of various hardness numbers (e.g., 7H and 6H). The coating was scratched using pencils of different hardness numbers and holding the pencil at an inclined angle of 45°. If pencils with a hardness higher than 5H made a scratch on the coating, the hardness of the coating was labeled 5H. The hardness range of pencils was from 9H (maximum hardness) to 6B (minimum hardness).

10) Open Circuit Potential

The coating was connected to a galvanostat/potentialstat as the working electrode. A saturated calomel electrode (SCE) was used as the reference electrode and platinum was used as the auxiliary electrode (or counter electrode) to stabilize the current. The open circuit potential between the working and reference electrodes was measured to estimate the thermodynamic tendency of the coating to undergo corrosion.

11) Immersion Test

The coatings were placed in a 3.0% NaCl solution for 90 d (for both the first and second stages). After 90-d immersion (for both the first and second stages), the visual inspection was performed to verify the appearance of the coating. The visual inspection included color change, coating deterioration, delamination, corrosion, expansion, cracks, softening, and other unsound characteristics.

12) Chemical Resistance Test

Coatings protected by the 4a5 mixture were placed in five environments for 240 h to evaluate their chemical resistance: 0.1M NaOH solution, 0.001M NaOH solution, 0.1M HCl solution, 0.001M HCl solution, and automobile gasoline. After immersion, the coating's adhesive capability was investigated using the X-cutting adhesive tape method, and its hardness was investigated using the pencil hardness test.

13) Weather Resistance Test (Ultraviolet Exposure)

The specimens were placed in a chamber of 160 cm (length) × 120 cm (width) × 80 cm (height), and 10 sets of 120-cm-long, 40-W ultraviolet light tubes were placed on the roof of the chamber. The distance between the ultraviolet light tubes was 11 cm. The walls of this chamber were covered by aluminum foil. After 90-d exposure, the coating was visually inspected to examine the following potential weather-induced changes: color changes, coating deterioration, delamination, corrosion, expansion, cracks, softening, and other unsound characteristics.

14) Scanning Electron Microscopy and Energy Dispersion Spectroscopy

Scanning electron microscopy (S-4800, Hitachi) was used to review the microscale structure of the coating. Energy dispersion spectroscopy was conducted to analyze the composition of the coating materials.

15) X-Ray Diffraction

X-ray diffraction (D-5000, Siemens) was performed to analyze the gray-colored chemical compounds formed in the immersion test.

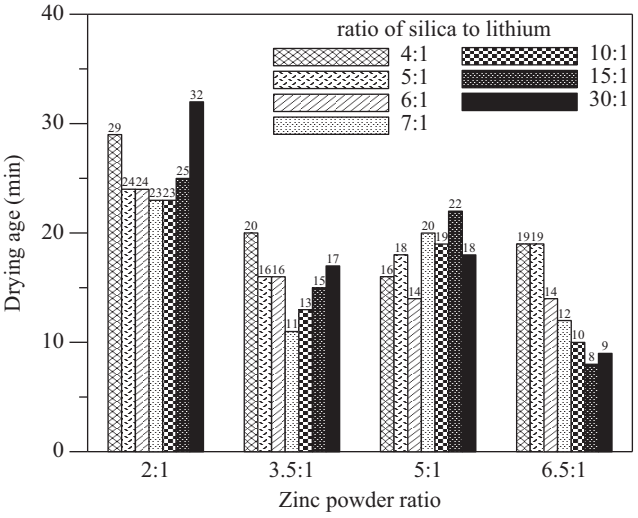

Fig. 2. Drying times for the various mixtures.

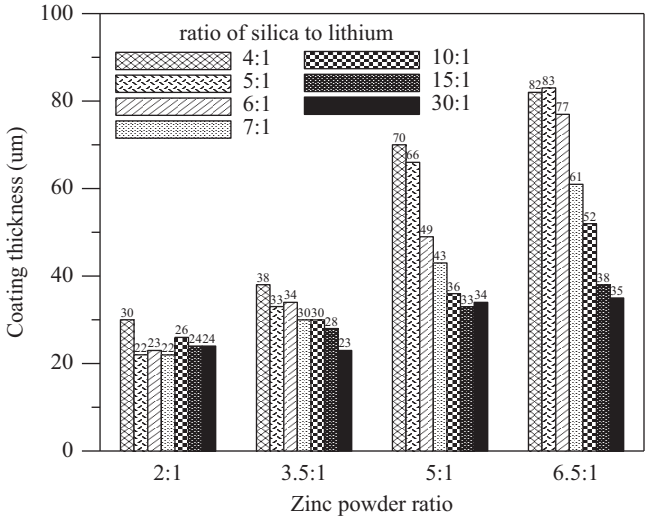

Fig. 3. Coating thickness for different mixtures.

III. RESULTS AND DISCUSSION

1. Workability and Film-Forming Ability

1) Drying Time

Fig. 2 shows the drying times for mixtures (different moduli and zinc powder ratios). For all mixtures, the coating hardened to reach the *half stiff and dry state* within 30 min, showing that the zinc-rich lithium silicate had a favorable hardening property. The drying time for the mixture of zinc powder ratio of 2:1 was higher than that for other mixtures, which implies that low quantities of zinc powder result in higher drying times. Only when the zinc powder ratio exceeds a specific value does the drying time difference become negligible. From Fig. 2, we can observe that when the zinc powder ratio exceeded 3.5:1, the drying time differences were not noticeable.

2) Thickness of Coatings

Fig. 3 shows the film thickness of the mixtures. The zinc powder ratio increased with film thickness because an increase in the amount of zinc powder led to an increase in the pile-up height (thickness). In addition, for mixtures with the same zinc powder ratio, film thickness increased as the modulus decreased. This pattern was found to be more pronounced as the zinc powder ratio increased, which may be explained as follows. The flowability of a mixture of high modulus is higher so that a lower amount of mixture is required with each brush stroke to attain the same workability. This resulted in lower film thickness with the same number of brush strokes on the plate. Furthermore, this pattern was found to be more significant as the zinc powder ratio increased. In general, when the zinc powder ratio increased, the workability of the brushing process decreased. Therefore, for mixtures with high zinc powder ratios, the difference between different moduli were more pronounced; the corollary is that for mixtures with high zinc powder ratios, the effect of using a lower modulus on the workability was more significant. Consequently, with the same number of brush strokes on the plate, the coating thickness was found to be higher for mixtures with poorer workability.

3) Appearance

For all mixtures with zinc powder ratios of 2:1 and 3.5:1, the appearance of the coatings was not acceptable because chaps and bursts were found and the coating could not be attached to the steel plate. When the zinc ratio was increased to 5:1, coating appearance was found to be smooth and uniformly distributed. When the amount of zinc powder was insufficient, the distance between particles was too high so that the binding force from the lithium silicate could not be overcome. Consequently, chaps and bursts occurred. When the zinc powder ratio was appropriate, the structure of the zinc pile up became dense such that the binding force from the lithium silicate was sufficient to maintain the integrity of the mixture. However, when the zinc ratio was increased to 6.5:1, the workability of the mixture decreased. Consequently, the surface exhibited some nonsmoothness. The aforementioned observations were true for all the moduli of silicate to lithium. The results reveal that the zinc powder ratio affected the appearance.

4) Mixing Capability and Workability

The mixing capability and workability passed the specifications of CNS 14132, except for the mixtures with a zinc powder ratio of 6.5:1. This result indicated that a high zinc powder ratio of 6.5:1 yielded a mixture that was not conducive to a manually brushing process, thereby leading to difficulties in the mixing process.

5) Flowability

The traveling times of the mixtures with a zinc powder ratio of 5:1 were recorded (see Fig. 4). As the moduli increased, the traveling time decreased, which meant that the flowability of the mixture increased. For a zinc powder ratio of 5:1, all the

Table 1. Results for adhesive tests for mixtures with zinc powder ratio of 5:1.

Mixture label	4a5	5a5	6a5	7a5	10a5	15a5	30a5
Pull-off strength (MPa)	2.02	2.28	2.22	2.65	3.00	3.30	3.12
Evaluation points from X-cutting tape method	8	2	0	0	0	0	0

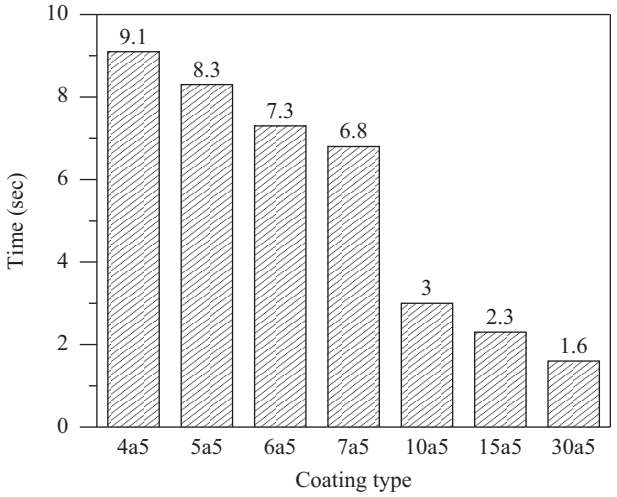

Fig. 4. Traveling times in the flowability tests for mixtures with a zinc powder ratio of 5:1.

mixtures satisfied mixing capability and workability requirements. However, high mixture flowability might not be suitable, especially for painting on overhead or vertical components.

2. Mechanical Behaviors

1) Adhesive Capability Tests

Table 1 shows the results of the X-cutting adhesive tape method and the pull-off strength test. The results of the X-cutting adhesive tape method show that as the moduli increased, the adhesive capability between the coating and the substrate (steel) decreased because of the high cohesive forces between the silica, which lead to cracks in the film. However, the results of the pull-off strength showed different trends. The inconsistent results can be explained as follows. A higher modulus may result in many microcracks in the coating. For the pull-off strength test, we must attach the steel head to the coating by using an adhesive agent. However, the adhesive agent itself had a high flowability, such that it penetrated into the defects of the coating, leading to an interlocking wedge effect, which enhanced the pull-off strength. Therefore, the pull-off strength tests does not represent the adhesive capability of the coating mixture to the substrate because defects existed in the system. The X-cutting adhesive tape method is recommended for evaluation of the adhesive capability of the coating material to the substrate.

2) Hardness

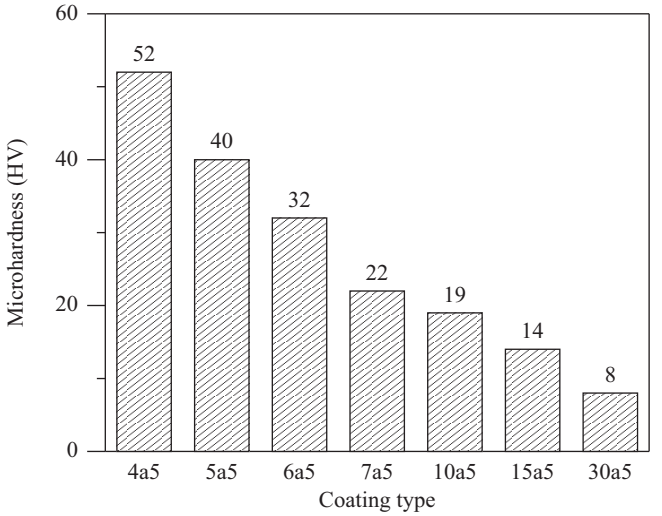

Fig. 5. Hardness values from the Vickers hardness test for mixtures with a zinc powder ratio of 5:1.

Fig. 5 shows the HV values for mixtures with a zinc powder ratio of 5:1. As the moduli *m* was increased, HV values decreased. This meant that the surface hardness of the coating decreased, a result that agrees with that obtained from the adhesive capability test using the X-cutting adhesive tape method. The reason for this result is that the high moduli mixture might result in coating microcracks, thus reducing the hardness value.

3. Corrosion Prevention Capability

1) First Stage

In this stage, the immersion tests for different mixtures were performed. During the immersion period, the coating and corrosion state of the steel was visually inspected. The open circuit potentials were monitored to check whether the sacrificial anode effect of the zinc powder could protect the steel plate. If the open circuit potential was lower than -800 mV (SCE), the steel was protected by the zinc-rich coating (Marchebois et al., 2002; Veritas, 2010).

From the visual inspection after 30-d immersion, mixtures 15a5 and 30a5 were found to carry red-colored rust, though the open circuit potentials were maintained at values greater than -800 mV (SCE). After 60-d immersion, all mixtures except the mixtures 4a5 and 5a5 showed corrosion signs (rust occurred and the open circuit potentials were higher than -800 mV [SCE]) and the sacrificial anode effect ceased.

Fig. 6 shows that as the immersion time increased, the open circuit potential increased for all the mixtures. The rate of increase of the open circuit potential was higher for the mixtures with higher moduli. The substrate, however, was found to be seriously corroded and the delamination phenomenon was more significant for mixtures with higher moduli. After 90-d immersion, the mixtures 4a5 and 5a5 alone had satisfactory corrosion prevention results. The open circuit potentials for the mixtures 4a5 and 5a5 were lower than -800 mV (SCE), implying a sacri-

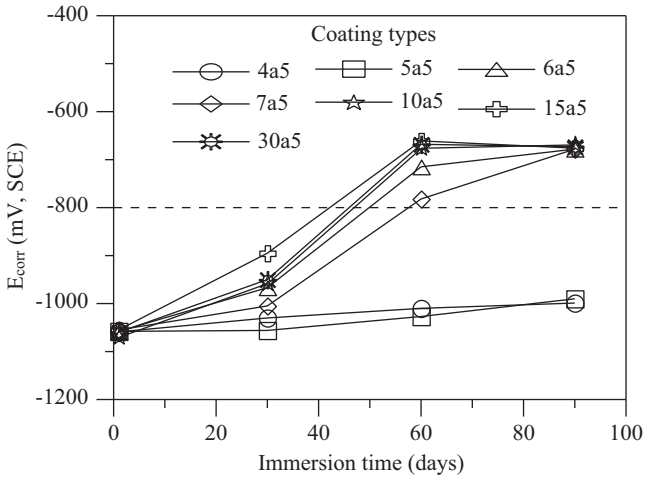

Fig. 6. Open circuit potentials for mixtures with a zinc powder ratio of 5:1.

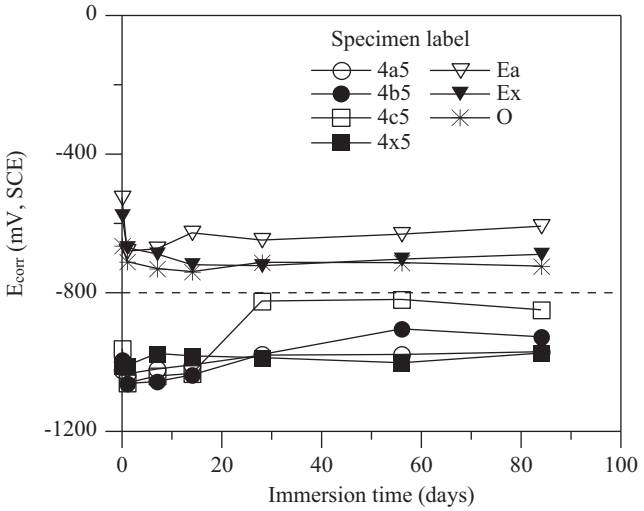

Fig. 7. Open circuit potentials for specimens in the second stage.

ficial anode effect of zinc powder. Red-colored rust was not to be found for these two mixtures. However, a little spalling was found on 5a5, as were traces of white zinc oxide. The appearance of 4a5 had a higher integrity and less white zinc oxide deposit.

2) Second Stage

On the basis of the results from the first stage, 4a5 was selected in the second stage. Different layers for the mixture 4a5 were considered as variables in this stage. In addition, X-shaped prescratched marks on the coatings were considered. The open circuit potential results for specimens protected by the 4a5 were compared with those of the specimen protected by epoxy coating and the specimen without protection (control specimen). Fig. 7 presents the open circuit potentials for the second stage tests.

We examined the corrosion prevention capabilities of the zinc-rich lithium silicate coating (for a zinc powder ratio of 5:1 and a modulus of 5) and the epoxy coating as well as their performance after an artificial scratch. The open circuit potentials 4a5 and 4x5 were similar, meaning that the zinc-rich lithium silicate coating provided excellent protection through the sacrificial anode effect from zinc powders even when a small area of scratch existed. By contrast, the epoxy coating exhibited poorer protection when the scratch existed. For epoxy coatings, a nobler potential means improved protection because the mechanism of protection originates from the physical barrier formed by the epoxy coating. When the epoxy coating retained its integrity, the open circuit potential was nobler than the corrosion potential of the steel plate. However, when the integrity of the epoxy coating was destroyed, the open circuit potential tended to have more active potential because some part of the steel plate encountered corrosion. From Fig. 7, we may infer that the open circuit potential for Ex was similar to that of the control specimen (O, without any protection). The corrosion of steel for the specimen Ex may be observed around the artificial scratch, whereas no significant signs of corrosion are found for 4a5 and 4x5. We may conclude that the zinc-rich lithium silicate coating can endure scratches for a limited region whereas the epoxy coating cannot.

As the number of layers increased, the corrosion prevention capability did not increase (see Fig. 7). After 90-dimmersion, we found that the appearance of 4b5 and 4c5 showed delamination of coating, which implies that more layers on the zinc-rich lithium silicate coating resulted in poor binding between layers. Consequently, the open circuit potentials for 4b5 and 4c5 tended to -800 mV (SCE) more quickly. After 30-d immersion, especially for 4c5, the open circuit potential rose dramatically and approached the marginal value. The preceding results suggest that the application of multiple layers of the zinc-rich lithium silicate coating is not recommended, a finding that requires further verification by future studies.

4. Chemical Resistance and Weather Resistance

1) Chemical Resistance

Table 2 summarizes the chemical resistance for 4a5, from which we may observe that the chemical resistance of the zinc-rich lithium silicate was insufficient in alkaline and acid environments. The corrosion rate for zinc increases in highly alkaline or highly acid environments (Roetheli et al., 1932). Therefore, the increasing corrosion rate of zinc powders led to the deteriorations of the surface. Zinc-rich lithium silicate, however, was found effective in a gasoline environment.

2) Weather Resistance (UV Exposure)

Over 90-d exposure in a UV exposure chamber, the color of the epoxy coating changed from light to dark yellow. The color change implied the existence of an undesirable change in the epoxy coating. These results reconfirmed the widely known fact that the UV resistance of epoxy is poor. No difference, however, was found between the specimens before and after UV exposure (protected by 4a5). The zinc-rich lithium silicate coating had a higher UV resistance compared with epoxy.

Table 2. Chemical resistance of zinc-rich lithium silicate coating.

Environments	Evaluation points from X-cutting adhesive tape method	Pencil hardness number	Surface status
0.1M NaOH	2	Lower than 5B	Pesting phenomenon on the surface by finger touching
0.001M NaOH	2	4H	Zinc oxide was found, and pesting phenomenon on the surface by finger touching
0.1M HCl	2	HB	Spalling
0.001M HCl	2	4H	Zinc oxide was found
Gasoline	8	Higher than 6H	No deterioration
Note: The evaluation point from the X-cutting adhesive tape method for the 4a5 mixture before immersion was 8, and the pencil hardness number before immersion was higher than 6H.			

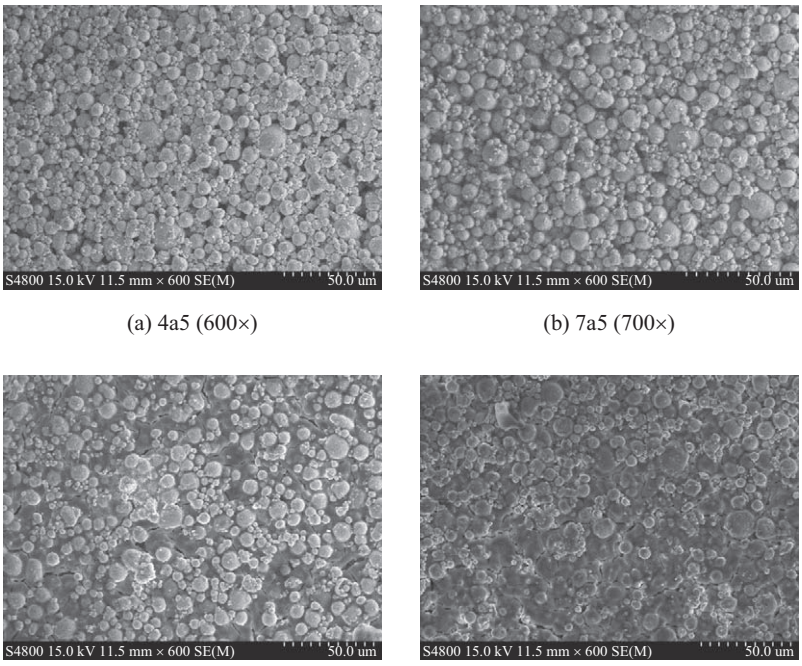

(a) 4a5 (600×) (b) 7a5 (700×)

(c) 15a5 (600×) (d) 30a5 (600×)

Fig. 8. Scanning electron microscopy images for the mixtures.

5. Microscale Experiments

1) Scanning Electron Microscopy and Energy Dispersive Spectroscopy

The scanning electron microscopy images for the 4a5, 7a5, 15a5, and 30a5 mixtures are shown in Figs. 8(a)-(d), respectively. As the modulus increased, so did the silica content. The cohesive force generated by the silicate was strong; and if the amount of silica increased, the cohesive force might result in film cracks. We observed from these figures that with a lower modulus, the coating retained its integrity. A high modulus resulted in cracks on the film. This finding explains the decrease in the mechanical strength of zinc-rich lithium silicate coating as the modulus increased.

Table 3 depicts the results of energy dispersive spectroscopy. As the table shows, the modulus increased, so did the silica content. The reason for the existence of carbon in the film is explained by the formation of the zinc-rich lithium silicate film (Parashar et al., 2001, 2003).

2) X-ray Diffraction

After the immersion test for the specimen using 4a5, the white deposit was analyzed using X-ray diffraction (see Fig. 9). The chemical composition of this white deposit was found to be ZnO and $Zn_5(OH)8Cl_2 \cdot H_2O$. The oxidation of zinc powder plays the role of the sacrificial anode so that the steel may be protected.

The study showed that the oxidation products of the zinc-rich lithium silicate film in a 3% NaCl solution are of two types, which differ from those obtained from air (in which the oxidation product is ZnO alone).

Table 3. Composition of various zinc-rich lithium silicate coatings (weight percentage)

Chemical / Component Label	C	O	Si	Zn	Total (Weight%)
4a5	15.47	15.66	1.21	67.66	100
7a5	14.48	21.58	3.96	59.49	
15a5	17.90	23.00	8.57	50.54	
30a5	10.49	30.89	14.33	44.30	

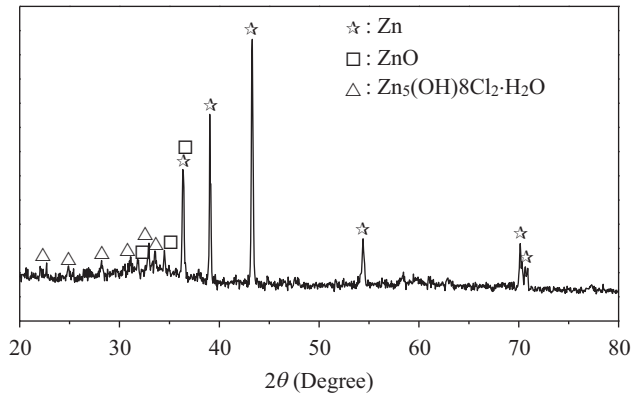

Fig. 9. X-ray diffraction results for the deposit formed by immersing the steel plate protected by 4a5 in a NaCl solution for 90 d.

IV. CONCLUSIONS

The main goal of this research was to determine the optimal moduli and zinc powder ratio. When the zinc powder ratio is greater than 3.5:1, the drying time is less than 20 min. Low zinc powder ratios result in deterioration, and high zinc ratios yield poor workability and mixing capabilities. Therefore, the zinc powder ratio must be carefully selected. Our experimental data suggest that a zinc powder ratio of 5:1 is optimal. The modulus affects the mechanical property and the corrosion prevention capability significantly. A lower modulus results in a film with improved mechanical properties (hardness or adhesive capability) and corrosion prevention capability. The optimal mixture of the zinc-rich lithium silicate in this study was that with a modulus of 4 and a zinc powder ratio of 5:1. This mixture was found to provide effective cathodic protection even when small-scale scratches existed on the film surface.

In addition, we found that increasing the number of coating layers failed to increase the corrosion prevention capability. This finding requires further verification by future studies.

The current experimental X-ray diffraction results showed that the oxidation products of zinc-rich lithium silicate coatings in different exposure environments (air or 3% NaCl solution) were different.

ACKNOWLEDGEMENTS

This work was supported by the National Science Council, Taiwan, under grant NSC 96-2622-E-109-004-CC3.

REFERENCES

Chen, Y. B., X. Y. Zhang, J. B. Dai and W. H. Li (2006). A new UV curable waterborne polyurethane: Effect of C=C content on the film properties. Progress in Organic Coatings 55(3), 291-295.

Canosa, G., P. V. Alfieri and C. A. Giudice (2012). Environmentally friendly, nano lithium silicate anticorrosive coatings. Progress in Organic Coatings 73(2-3), 178-185.

Cruz, D., S. Bulbulian, E. Lima and H. Pfeiffer (2006). Kinetic analysis of the thermal stability of lithium silicates (Li_4SiO_4 and Li_2SiO_3). Journal of Solid State Chemistry 179(3), 909-916.

Giudice, C. A. (2012). Reinforcement fibers in zinc-rich nano lithium silicate anticorrosive coatings. In Corrosion Resistance, edited by H. Shih. (Chapter 7, 157-174), published by InTech.

Hammouda, N., H. Chadli, G. Guillemot and K. Belmokre (2011). The corrosion protection behaviour of zinc rich epoxy paint in 3% NaCl solution. ACES 1(2), 51-60.

Hare, C. H. (1998). Paintindia 48(4), 47.

Jegannathan, S., T. S. Narayanan, K. Ravichandran and S. Rajeswari (2006). Formation of zinc phosphate coating by anodic electrochemical treatment. Surface and Coatings Technology 200(20-21), 6014-6021.

Kumar, R., A. Arvind, M. Goswami, S. Bhattacharya, V. K. Shrikhande and G. P. Kothiyal (2009). The effect of NiO on the phase formation, thermophysical properties and sealing behaviour of lithium zinc silicate glass-ceramics. Journal of Materials Science 44(13), 3349-3355.

Marchebois, H., S. Touzain, S. Joiret, J. Bernard and C. Savall (2002). Zinc-rich powder coatings corrosion in sea water: influence of conductive pigments. Progress in Organic Coatings 45(4), 415-421.

Oostendorp, D. J., G. L. Bertrand and J. O. Stoffer (1992). Kinetics and mechanism of the hydrolysis and alcoholysis of alkoxysilanes. Journal of Adhesion Science and Technology 6(1), 171-191.

Parashar, G., D. Srivastava and P. Kumar (2001). Ethyl silicate binders for high performance coatings. Progress in Organic Coatings, 1-14.

Parashar, G., M. Bajpayee and P. K. Kamani (2003). Water-borne non-toxic high-performance inorganic silicate coatings. Surface Coatings International Part B: Coatings Transactions 86(3), 209-216.

Pfeiffer, H., P. Bosch and S. Bulbulian (1998). Synthesis of lithium silicates. Journal of Nuclear Materials 257(3), 309-317.

Pedersen, L. T., C. Weinell, A. S. Hempel, P. Verbiest, J. Van Den Bosch and J. Umicore (2009). Advancements in high performance zinc epoxy coatings Zinc. Chemicals Source Corrosion, Copyright NACE International.

Roetheli, B. E., G. L. Gox and W. B. Littreal (1932). Effect of pH on the corrosion products and corrosion rate of zinc in oxygenated aqueous solutions. Metals and Alloys 3, 73-76.

Sidkey, P. S. and M. G. Hocking (1999). Review of inorganic coatings and coating processes for reducing wear and corrosion. British Corrosion Journal 34(3), 171-183.

Sorensen, P. A., S. Kiil, K. Dam-Johansen and C. E. Weinell (2011). Anticorrosive coatings: a review, Chemistry and Materials Science. Journal of Coatings Technology and Research 6(2), 135-176.

Veritas, D. N. (2010). Cathodic protection design. Recommended Practice DNV-RP-B401, Copyright Det Norske Veritas.

Weldes, H. H. and K. R. Lange (1969). Properties of soluble silicates. Industry Engineering Chemistry 61(4), 29-44.